Transactions of JASCOME, Vol. 3 (July 2003), Paper No. 03-062009 **JASCOME**

EVALUATION OF HEAT CONDUCTING PROPERTIES OF CURVED-CNT COMPOSITES BY THE HYBRID BNM

Masataka TANAKA [1)], Jianming ZHANG [2)], Toshiro MATSUMOTO [3)] , Artur GUZIK [4,*)]

1) Faculty of Engineering, Shinshu University, (Nagano 380-8553, e-mail: dtanaka@gipwc.shinshu-u.ac.jp)

2) Faculty of Engineering, Shinshu University, (Nagano 380-8553, e-mail: zhangjm@homer.shinshu-u.ac.jp)

3) Faculty of Engineering, Shinshu University, (Nagano 380-8553, e-mail: toshiro@gipwc.shinshu-u.ac.jp)

4) Faculty of Engineering, Shinshu University, (Nagano 380-8553, e-mail: guzik@homer.shinshu-u.ac.jp)

* On leave from Cracow University of Technology, Cracow, Poland

Carbon nanotubes (CNT) are predicted to possess superior heat conductivity and considerably improve heat conducting properties of polymers. In this work, the equivalent heat conductivities of CNT-based nanocomposites with curved CNTs are evaluated. A 3-D nano-scale representative volume element (RVE) model is used and, as a solution technique, the hybrid boundary node method (HBNM) employed. Both the temperature distribution and heat flux concentration are studied. The equivalent heat conductivity of the RVE as a function of the nanotube curvature is calculated and discussed in detail. It is found that, unlike the mechanical properties, the nanotube curvature has no significant influence on the equivalent heat conductivity of the composites.

Keywords: Carbon Nanotube, Meshless Method, Nanocomposite, Heat Conductivity, Hybrid Boundary Node Method

1. Introduction

Over the last decade, carbon nanotubes have been attracting considerable attentions both from scientists and engineers. Intensive research has been carried out on carbon nanotubes for their production, physical properties and possible applications [1]. The carbon nanotubes are predicted to possess exceptional physical properties such as superior heat and electrical conductivities, as well as high stiffness and strength. A few recent experiments have been reported on mats of compressed ropes of CNTs [2], from which values of thermal conductivity of CNTs ranging from 1750 to 5850 W/m·K have been extrapolated. The direct measurements of individual nanotube were also tried with the MEMS assisted new measurement technology [3]. Following those experiments, several preliminary molecular dynamics simulations of the thermal conductivity gave even higher values, namely 6600 W/mK at 300 K [4]. Although the estimated values of thermal conductivity were different from each other, it is generally accepted that the CNTs possess excellent heat conductivity comparable or even better than diamond, considered so far as the best heat conductor.

These remarkable properties of CNTs may make them ideal for a wide variety of technological applications. One of the most intriguing applications is the use of CNT as a small volume fraction filler in nanotube-reinforced polymers. CNT-based composites offer significant improvements in performance over their base polymers. It has been demonstrated that with only 1% (by weight) of CNTs added in a matrix material, the stiffness of a resulting composite can increase between 36% and 42% and the tensile strength by 25% [5].

CNTs are different in sizes and forms when they are dispersed in a matrix to make a nanocomposite. They can be single-walled or multi-walled with length of a few nanometers to a few micrometers, and can be straight, twisted and curled, or in the form of ropes. Their distribution and orientation in the matrix can be uniform and unidirectional or random. All these factors may substantially influence the equivalent properties of the nanocomposites.

A critical issue that has yet to be examined is the impact of the shape of the embedded nanotube on the effective properties of the nanotube-reinforced polymer. Using the FEM, Fisher et al. [6] analyzed the effects of the nanotube waviness on the modulus of the nanocomposite through a RVE with a curved nanotube. They found that the nanotube curvature significantly reduces the effective reinforcement when compared to straight nanotubes.

In this paper, we focus on thermal property of the CNT-based composites. We also use a representative unit volume with a curved nanotube embedded to assess the impact of nanotube waviness on the equivalent heat conductivity of the nanocomposites.

The implementation of standard numerical solution techniques like FEM or BEM may face severe difficulties in discretization of the domain geometry under consideration. This is valid especially for FEM models where meshing of the solid geometries within CNT-reinforced polymers may be (and usually is) tedious and extremely difficult. To alleviate this difficulty the hybrid boundary node method (HBNM) can be used [7-8]. By combining a modified functional with the moving least squares (MLS)

approximation, the HBNM is a truly meshless, boundary-only method. The HBNM requires only discrete nodes located on the surface of the domain and its parametric representation. As the parametric representation of created geometry is used in all CAD packages, it should be possible to exploit their *Open Architecture* features and handle truly arbitrary geometry. (For full details of HBNM refer to [7]). In the following section, for completeness, a very brief overview of multi-domain HBNM is given.

2. HBNM for multi-domain models

For the sake of simplicity, two domains, i.e. the nanotube and the polymer, are considered here. It is assumed that both the CNT and the matrix in the RVE are continua of linear, isotropic and homogenous materials with given heat conductivities. A steady-state heat conduction problem governed by Laplace's equation with proper boundary conditions is considered for each domain.

The hybrid boundary node method is based on a modified variational principle, in which there are three independent variables, namely:

– temperature within the domain, ϕ;

– boundary temperature, $\tilde{\phi}$;

– boundary normal heat flux, $\tilde{q}$.

Suppose that N nodes are randomly distributed on the bounding surface of a single domain. The domain temperature is approximated using fundamental solutions as follows:

$$\phi = \sum_{I=1}^{N} \phi_I^s x_I \,, \tag{1}$$

and hence at a boundary point, the normal heat flux is given by:

$$q = -\kappa \sum_{I=1}^{N} \frac{\partial \phi_I^s}{\partial n} x_I \,, \tag{2}$$

where ϕ_I^s is the fundamental solution with the source at a node $\mathbf{s}_I$, κ is the heat conductivity and x_I are unknown parameters. For 3-D steady state heat conduction problems, the fundamental solution can be written as

$$\phi_I^s = \frac{1}{\kappa} \frac{1}{4\pi r(Q, \mathbf{s}_I)}, \tag{3}$$

where Q is a field point; $r(Q,\mathbf{s}_I)$ is the distance between the point Q and the node $\mathbf{s}_I$.

The boundary temperature and normal heat flux are interpolated by the moving least square (MLS) approximation:

$$\tilde{\phi}(\mathbf{s}) = \sum_{I=1}^{N} \Phi_I(\mathbf{s}) \hat{\phi}_I \,, \tag{4}$$

and

$$\tilde{q}(\mathbf{s}) = \sum_{I=1}^{N} \Phi_I(\mathbf{s}) \hat{q}_I \,. \tag{5}$$

In the foregoing equations, $\Phi_I(\mathbf{s})$ is the shape function of MLS approximation; $\hat{\phi}_I$ and $\hat{q}_I$ are nodal values of temperature and normal flux, respectively.

For the polymer domain, the following set of equations, expressed in matrix form, are given:

$$\begin{bmatrix} U_{00}^p & U_{01}^p \\ U_{10}^p & U_{11}^p \end{bmatrix} \begin{Bmatrix} x_0^p \\ x_1^p \end{Bmatrix} = \begin{Bmatrix} H_0^p \hat{\phi}_0^p \\ H_1^p \hat{\phi}_1^p \end{Bmatrix}, \tag{6}$$

$$\begin{bmatrix} V_{00}^p & V_{01}^p \\ V_{10}^p & V_{11}^p \end{bmatrix} \begin{Bmatrix} x_0^p \\ x_1^p \end{Bmatrix} = \begin{Bmatrix} H_0^p \hat{q}_0^p \\ H_1^p \hat{q}_1^p \end{Bmatrix}, \tag{7}$$

where superscripts p, 0 and 1 stand for polymer, quantities exclusively associated with a domain, and quantities associated with the interface, respectively. The sub-matrices $[U]$, $[V]$ and $[H]$ are defined as:

$$U_{IJ} = \int_{\Gamma_s^J} \phi_I^s v_J(Q) d\Gamma \,, \tag{8}$$

$$V_{IJ} = \int_{\Gamma_s^J} q_I^s v_J(Q) d\Gamma \,, \tag{9}$$

$$H_{IJ} = \int_{\Gamma_s^J} \Phi_I(\mathbf{s}) v_J(Q) d\Gamma \,, \tag{10}$$

where v_J is a weight function and $\mathbf{s}$ is a boundary point, Γ_s^J is a regularly shaped local region around a given node $\mathbf{s}_J$ in the parametric representation space of the boundary surface. Therefore, the integrals in equations (8), (9) and (10) can be computed without using boundary elements. (For details refer to [7]).

Similarly, for the nanotube domain we have:

$$\begin{bmatrix} U_{00}^n & U_{01}^n \\ U_{10}^n & U_{11}^n \end{bmatrix} \begin{Bmatrix} x_0^n \\ x_1^n \end{Bmatrix} = \begin{Bmatrix} H_0^n \hat{\phi}_0^n \\ H_1^n \hat{\phi}_1^n \end{Bmatrix}, \tag{11}$$

and

$$\begin{bmatrix} V_{00}^n & V_{01}^n \\ V_{10}^n & V_{11}^n \end{bmatrix} \begin{Bmatrix} x_0^n \\ x_1^n \end{Bmatrix} = \begin{Bmatrix} H_0^n \hat{q}_0^n \\ H_1^n \hat{q}_1^n \end{Bmatrix}, \tag{12}$$

where the superscript n stands for the nanotube.

As the continuity and equilibrium conditions at the interface between the nanotube and the polymer must be satisfied, i.e.

$$\{\phi_1^p\} = \{\phi_1^n\} \tag{13}$$

and

$$\{q_1^p\} = -\{q_1^n\}, \tag{14}$$

equations (6), (7), (11) and (12) can be assembled into the following expression:

$$\begin{bmatrix} A_{00}^p & A_{01}^p & 0 & 0 \\ U_{10}^p & U_{11}^p & -U_{10}^n & -U_{11}^n \\ V_{10}^p & V_{11}^p & V_{10}^n & V_{11}^n \\ 0 & 0 & A_{00}^n & A_{01}^n \end{bmatrix} \begin{Bmatrix} x_0^p \\ x_1^p \\ x_0^n \\ x_1^n \end{Bmatrix} = \begin{Bmatrix} H_0^p d_0^p \\ 0 \\ 0 \\ H_0^n d_0^n \end{Bmatrix}, \tag{15}$$

where $[A_{00}^p]$, $[A_{01}^p]$ and $\{d_0^p\}$ are formed by merging $[U_{00}^p]$ and $[V_{00}^p]$, $[U_{01}^p]$ and $[V_{01}^p]$, and $\{\hat{\phi}_0^p\}$ and $\{\hat{q}_0^p\}$, respectively, according to the known boundary conditions. For degrees of freedom with prescribed temperature, the related elements in $\{\hat{\phi}_0^p\}$ are selected for $\{d_0^p\}$, and the corresponding rows of $[U_{00}^p]$ and $[U_{01}^p]$ are selected for $[A_{00}^p]$ and $[A_{01}^p]$; otherwise, elements in $\{\hat{q}_0^p\}$ are selected for $\{d_0^p\}$, and the corresponding rows in $[V_{00}^p]$ and $[V_{01}^p]$ are selected for $[A_{00}^p]$ and $[A_{01}^p]$. In the same way, $[A_{00}^n]$,

$\left[A_{01}^n\right]$ and $\left\{d_0^n\right\}$ are formed by merging $\left[U_{00}^n\right]$ and $\left[V_{00}^n\right]$, $\left[U_{01}^n\right]$ and $\left[V_{01}^n\right]$, and $\left\{\hat{\phi}_0^n\right\}$ and $\left\{\hat{q}_0^n\right\}$, respectively.

The set of Eqs. (15) is solved for unknown parameters $\boldsymbol{x}$, and then, by back-substitution into equations (6), (7), (11) and (12), the boundary unknowns are obtained either on the interface or the external boundary. As demonstrated, the HBNM is a boundary-only meshless approach. No boundary elements are used for either interpolation or integration purposes. Therefore, it can alleviate the discretization difficulty to a large extent.

3. Numerical results

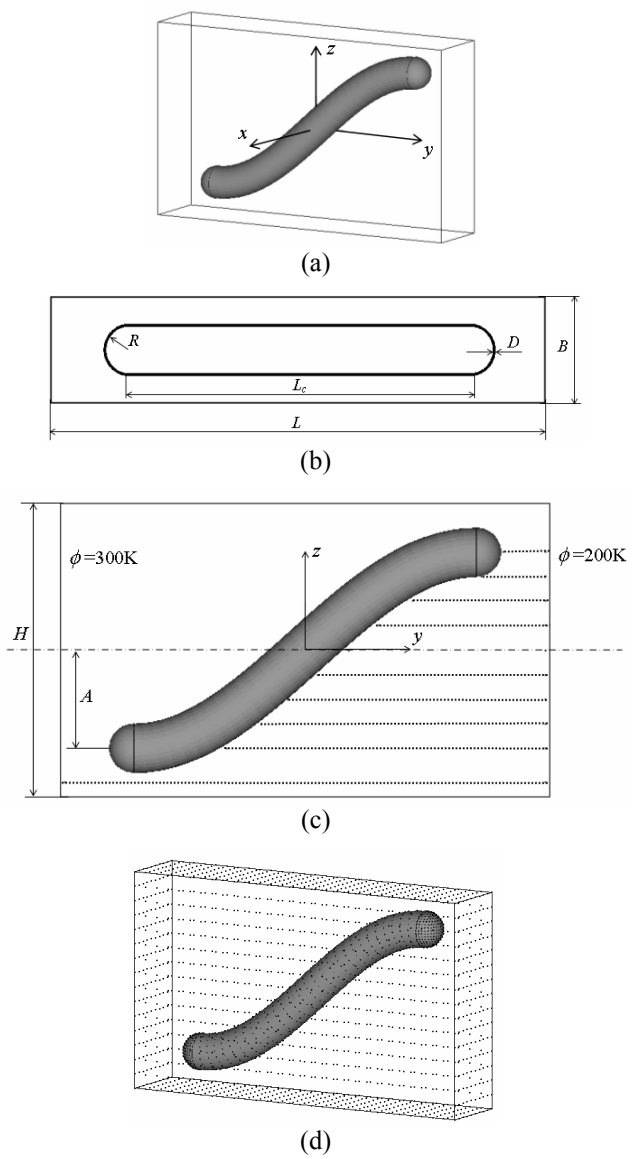

Fig.1 Nanoscale representative volume element with a curved nanotube inside. (a) The unit model and coordinates system; (b) Top view: dimensions; (c) Side view: dimensions, boundary conditions and results output locations; (d) Discretisation with boundary nodes.

In order to study the effect of CNT waviness and its influence on thermal properties of nano-composites, the unit RVE model with the curved CNT embedded is used. The geometry and boundary conditions are presented in Fig. 1 (a-c). Fig. 1 (d) shows the computational model discretised with boundary nodes.

Nanotube waviness is considered by prescribing a sinusoidal NT shape as:

$$z = A\sin\left(\frac{2\pi y}{L_c}\right), \tag{16}$$

where L_c stands for the wave length of the sinusoid function, and y is the fiber axial direction.

Homogeneous boundary conditions are considered here, namely uniform temperatures of 300K and of 200K imposed at the two end faces of the RVE, respectively, and heat flux free at all other faces of the RVE and the inner face of the CNT cavity. This boundary condition set allows us to estimate equivalent heat conductivity of CNT-based composite in the axial direction. Assuming homogeneous material properties and using Fourier's law, the formula for equivalent heat conductivity can be written as

$$\kappa = -\frac{qL}{\Delta\phi}, \tag{17}$$

where κ represents the heat conductivity; q is the heat flux density, L the length of the RVE in the axial direction and $\Delta\phi$ the temperature difference between the two end faces.

3.1 Temperature and fluxes distributions in an RVE with a curved CNT

First, an RVE for a curved CNT of a specific length and waviness is studied. The dimensions of the RVE are: for the matrix, length L=100 nm, B=20 nm and H=60 nm; for the CNT, length L_c=70 nm, A=20 nm outer radius R=5 nm, thickness D=0.4 nm (which is close to the theoretical value of 0.34 nm for SWCNT thickness). The heat conductivities used for the CNT and matrix (Polycarbonate) are

CNT: $\kappa^t = 6000$ W/m·K;

Matrix: $\kappa^m = 0.19$ W/m·K.

These values are within the wide range of dimensions and material constants for CNTs reported in literature [1-11].

It is worth emphasizing that: (i) the thickness of the CNT is very small; and (ii) the difference of heat conductivity between the CNT and the matrix is extremely large. In this simulation, 2208 nodes are used for the CNT and 2984 nodes for the matrix (see Fig. 1 (d).

The temperature distribution and heat flux in the axial direction (along the dotted lines in Fig. 1 (c)) are presented in Fig. 2. An obvious feature of the temperature distribution is observed in Fig.2 (a) that the temperatures at the locations close to CNT (the start points for each dotted line except the one that passes all through the matrix) are almost uniform. This observation is consistent with the physical interpretation. As the heat conductivity of the CNT is several orders of magnitude higher than that of the matrix, almost the entire flux flows through the CNT. Therefore, nearly no flux flows in the matrix at the locations near the central part of the CNT, and the temperature at these locations is almost uniform. The corresponding heat flux concentrations are also observed near the tip of the CNT (z = 20) in Fig. 2 (b). The heat fluxes in the matrix at the locations near the middle part of the CNT are very small and approaching zero.

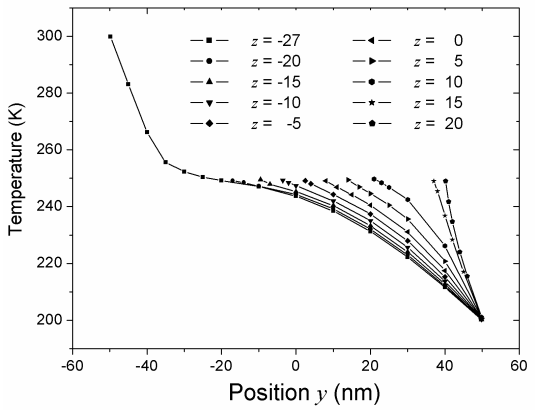

(a)

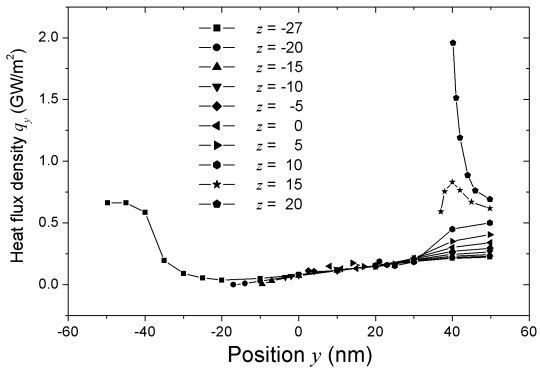

(b)

Fig.2 Temperature and heat flux distribution in the matrix.

3.2 Equivalent constants of composites with various CNT waviness

The influence of CNT waviness on the equivalent material constant, employing several models with various CNT waviness ratios, is also investigated. Dimensions and parameters of Section 3.1 are kept, except for the waviness ratio (w=A/L_c) and the ratio of the phase constant ($C_r = \kappa^{CNT} / \kappa^{matrix}$). The waviness ratio is changed by varying the amplitude A of the sinusoid curve while keeping the half waviness L_c constant. Computations were performed for the following phase constant ratios: C_r=30000, C_r=300 and C_r=30. For each value of C_r the conductivity of the matrix is held constant at 0.19 W/m·K. The equivalent heat conductivity of the RVE as a function of w is presented in Fig.3. Results demonstrate that equivalent heat conductivity is only slightly dependent on the CNT waviness for both high and low ratios of the phase conductivity. These results are in sharp contrast to that of the elasticity problem [6].

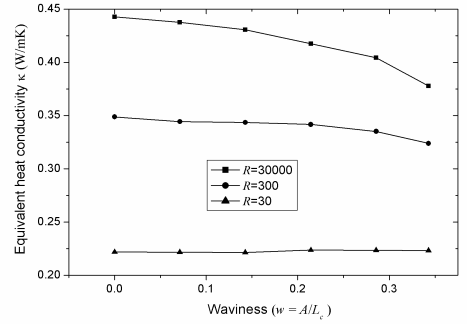

Fig.3 Equivalent heat conductivity for various waviness.

Conclusions

In this paper, an RVE of CNT-based composites with a curved CNT inside it has been studied. It was demonstrated that temperatures within the CNT and at the interface are almost uniform, and heat flux concentration occurs at the two tips of the CNT. The effects of the CNT waviness on the equivalent conductivity were also investigated. Contrary to the elastostatics case [6], the presented results show that the equivalent heat conductivity is less affected by the waviness of the CNT.

The results and models presented in this paper should be considered only as the first step in evaluating the equivalent thermal properties of the CNT-based nanocomposites. Naturally, further improvements of the model are required, as thermophysical properties of randomly scattered CNTs are obviously of importance and must be accounted for. This challenging task may be accomplished by coupling the HBNM with the fast multipole method [9]. This is a subject of ongoing research.

Acknowledgements

This work was supported by the CLUSTER of Ministry of Education, Culture, Sports, Science and Technology (Japan).

References

1. Endo, M., Kim, Y.A., Hayashi, T., Nishimura, K., Matushita, T., Miyashita, K. and Dresselhaus, M.S., Vapor-grown carbon fibers (VGCFs): Basic properties and their battery applications, *Carbon*, **39** (2001), pp. 1287-1297.
2. Hone, J., Whitney, M., Piskoti, C., and Zettl, A., "Thermal conductivity of single-walled nanotubes," *Phys. Rev. B*, Vol. 59, No. 4 (1999), pp. 2514–2516.
3. Kim, P., Shi, L., Majumdar, A., and McEuen, Pl., Thermal transport measurements of individual multiwalled nanotubes, Phys. Rev. Lett., 87 (2001), 215502-1.
4. Berber, S., Kown, Y.-K., and Tomanek, D., Unusually high thermal conductivity of carbon nanotubes, *Phys. Rev. Let.*, Vol. 84, No. 20 (2000), pp. 4613–4617.
5. Qian, D., Dickey, E.C., Andrews, R., Rantell, T., Load transfer and deformation mechanisms in carbon nanotube polystyrene composites, Applied Physics Letters, Vol. 76, No. 20 (2000), pp. 2868–2870.
6. Fisher, F.T., Bradshaw, R.D., Brinson, L.C., Effects of nanotube waviness on the modulus of nanotube-reinforced polymers, Applied Physics Letters, Vol. 80, No. 24 (2000), pp. 4647–4649.
7. Zhang, J.M., Yao, Z.H., Li, H., A hybrid boundary node method, International Journal for Numerical Methods in Engineering, Vol. 53 (2002), pp. 751-763.
8. Zhang, J.M., Tanaka, M., Matsumoto, T., Meshless analysis of potential problems in three dimensions with the hybrid boundary node method, International Journal for Numerical Methods in Engineering, submitted.
9. Nishida, T., and Hayami, K., Application of the fast multipole method to the 3D BEM analysis of electron guns, In Marchettia, M., Brebbia, C.A., and Aliabadi, M.H., Eds., *Boundary Elements XIX*, Computational Mechanics Publications (1997), pp. 613–622.